Rigorous Synthesis and Simulation of Complex Distillation Networks

Gerardo J. Ruiz, Seon B. Kim, Laura Moes, and Andreas A. Linninger
Dept. of Chemical Engineering and Bioengineering, Laboratory for Product and Process Design, University of Illinois at Chicago, Chicago, IL 60607

DOI 10.1002/aic.12245
Published online April 20, 2010 in Wiley Online Library (wileyonlinelibrary.com).

Recent insights for better understanding the thermodynamic foundations of separation processes have renewed the interest in exploring energy-efficient distillation networks. Complex column networks have substantial potential for energy savings over conventional configurations. This article introduces a computational algorithm for synthesizing such complex energy-efficient networks. A robust feasibility criterion drives the selection of design specification and operating conditions. It will be shown that columns composed of sections whose liquid stage composition profiles have no gaps are realizable. To prove the rigor of design computations, numerous separation networks were synthesized and validated with the Aspen flowsheet simulator. By using our computational results as input, AspenPlus simulations converged in a few iterations. Our method builds on temperature collocation, a thermodynamically motivated search method for determining feasible operating conditions and design details for achieving the desired product targets. Our findings suggest that significant energy savings can be realized with rigorous complex networks synthesis for industrial separation problems.
 AIChE J, 57: 136–148, 2011
Keywords: complex column, networks, temperature collocation, inverse design, Aspen validation

Introduction

Distillation continues to be the most widely used separation technique in the chemical and petrochemical industry. Although distillation requires heat, it still remains a simple and economic way to separate many multicomponent liquid mixtures.

Recently, advancements in design and synthesis of separation systems slowly do away with the myth that distillation is a mature and thermally optimized technology. We will review the most relevant work related to this study. Doherty and coworkers[1,2] developed the boundary value method based on the intersection of stripping and rectifying profiles in the continuous stage number space. Marquardt[3] proposed the use of rectifying bodies, which are constructed by connecting the pinch points belonging to column sections. According to this method, intersection of the rectifying bodies between two adjacent rectifying and stripping column sections implies feasibility. Yet, realizable column profiles are not necessarily confined in the convex hull spanned by rectifying bodies, nor do pinch points always come to lie in real space so as to form a convex geometric object.[4]

Agrawal and Fidkowski[5] proposed a strategy to develop structural alternatives for complex and simple distillation networks. Another important advancement is Agrawal's procedure for the exhaustive enumeration of complex flowsheets.[6] They systematically evaluated the energy consumption of so called basic feasible configurations of complex networks and advocate the energy savings that can potentially be achieved through feasible thermal coupling. Their

Correspondence concerning this article should be addressed to A. A. Linninger at linninge@uic.edu.

complete synthesis of candidate flowsheet structures is an important step for a fully automatic separation synthesis.

Lucia and Taylor[7,8] studied composition trajectories related to stationary points and residual composition maps to understand the separation path in different boundary regions of composition planes. Recently, they propose a new approach based on the concept of shortest stripping line distance to identify minimum energy requirements by minimizing the length of the stripping profile.[9]

Glasser and Hildebrandt[4,10] developed a design technique using generalizing column section computations giving rise to column profile maps encompassing all realizable liquid composition profiles for simple as well as complex column sections. This concept is closely related to residue curve maps and can be applied for assessing feasible separations.

Zhang and Linninger developed a novel composition model approach called temperature collocation, replacing the conventional tray number by the bubble point temperature.[11] This thermodynamic variable transformation drastically reduces the design search space, because this absolute bubble point temperature is independent of stage numbers and applies to both stripping and rectifying sections. Every new stage computation which traditionally opens new search dimensions for its number of stages or section length can be transformed onto a global and characteristic temperature scale. This efficient and reliable computational algorithm based on a bubble point distance criterion, BPD, can establish the feasibility or impossibility of realizing desired product specifications for sharp or sloppy separations of multicomponent mixtures using ideal, nonideal, or azeotropic vapor–liquid equilibrium models. The BPD criterion was previously applied successfully for the automatic synthesis of simple column networks.[12,13]

This article describes the extension of the BPD criterion for the design and synthesis of complex column network configurations. The paper is organized as follows: First, a methodology for the exhaustive synthesis of complex separations trains will be introduced. Results and applications demonstrate the rigorous design and analysis of networks of simple and complex columns to separate a quaternary mixture into almost pure products. The importance of nonsharp, nonpinched column sections for energy efficiency will be highlighted. All structural alternatives will be evaluated and designed in detail using the temperature collocation algorithm. All inverse design problem solutions are validated using an industrial flowsheet simulator AspenPlus, thereby demonstrating the versatility and robustness of our inverse design algorithm to solve realistic industrial separation problems. Finally, this article ends with a brief discussion and conclusions.

Methodology

Network synthesis

Forward simulation also known as performance calculations is a popular technique for distillation process design. However, for difficult separation tasks, it is time consuming and requires experience to specify key input variables such as feed composition, feed and product flow rates, feed thermodynamic state, and column design parameters like number of stages, feed stages, and reflux ratios. If any of these parameters is assigned improperly, the flowsheet simulation may fail to converge. On the other hand, the inverse design problem asks whether a desired product target can be reached with any network configuration with suitable operating conditions. This inverse design is harder to solve than the performance problem, but has the advantage that it can be used to detect infeasible specifications. For complex column networks, the rigorous inverse design problem has the following requirements.

(i) Configurations should incorporate any combination of simple and complex column sections such as prefractionators or Petlyuk or Kaibel designs.

(ii) Column profile equations model should admit all liquid–vapor phase equilibrium relationships such as constant relative volatility, ideal, nonideal, and azeotropic mixtures.

(iii) In feasible designs, liquid composition profiles must exactly intersect meaning that trajectories of the liquid compositions connect continuously all product streams from the top to the bottom. On the other hand, infeasible design specification should easily be identifiable by a gap in at least one pair of composition profiles in adjacent column sections.

These considerations have led to a novel inverse design methodology based on temperature collocation. The methodology has two main elements reviewed briefly in the next subsection: (i) rigorous profile computations and (ii) bubble point distance for a network feasibility criterion. A brief review of the main basics of temperature collocation is introduced next, the mathematical background is given briefly in the Appendix. A detail derivation of the theoretical basis of finite element collocation and its application for temperature collocation is beyond the scope of this article, but is discussed in depth in a previous publication.[11]

Rigorous profile computations

The generalized column profile equations discovered by Glasser and Hildebrand[4,10] describe the evolution of liquid composition profiles along the column length, n, as in Eq. 1 in terms of the generalized reflux, R_Δ, and the difference point composition for component j in the multicomponent mixture, $X_{\Delta j}$. The difference point composition of the j-species, $X_{\Delta j}$, is equal to the distillate or bottom composition in conventional stripping or rectifying sections. In complex sections—not producing a single product—it can be interpreted as the concentration difference between the vapor and liquid stream leaving the section. In this sense, $X_{\Delta j}$, ensures the operating line conditions in the same way the product purities normally do. The generalized reflux, R_Δ, is the recirculation ratio belonging to a column section, with a role similar to the reflux in conventional columns. The difference point equation also applies to simple column sections, thus rendering a single mathematical expression for all sections in any separation network whether they are complex or simple.

$$\frac{dx_j}{dn} = \left(1 + \frac{1}{R_\Delta}\right)(x_j - y_j) + \frac{1}{R_\Delta}(X_{\Delta j} - x_j)$$

with

$$R_\Delta = L/\Delta \;\; X_{\Delta j} = (Vy_j - Lx_j)/\Delta. \tag{1}$$

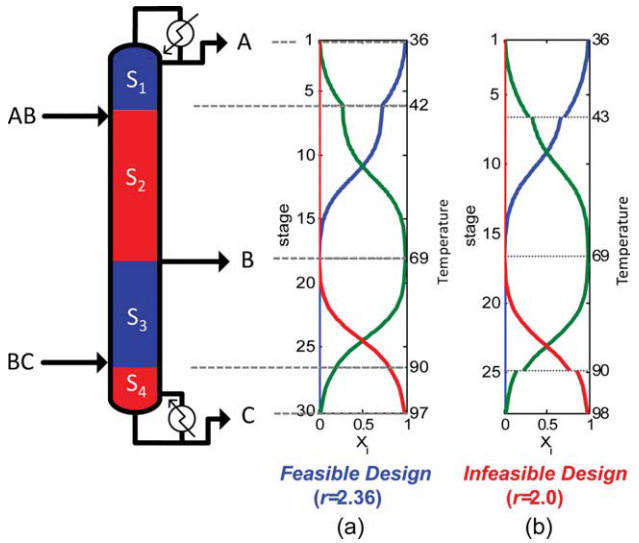

Figure 1. Complex column with four sections S1–S4 for the separation of mixture of three species *A* (blue), *B* (green), and *C* (red).

Frame (a) depicts the liquid composition profiles along the number of stages (left ordinate) and the equivalent bubble point temperature (right ordinate) for a reflux $r = 2.36$. This design is feasible, because the profiles have zero bubble point distance. Frame (b) plots the liquid composition profiles for a different reflux of $r = 2$. This design is infeasible, because the composition trajectories have discontinuities between adjacent section pairs S_1–S_2; as well as S_3–S_4. [Color figure can be viewed in the online issue, which is available at wileyonlinelibrary.com.]

Here, x_j is the liquid composition, y_j is the vapor composition, n is the number of stages, and $\Delta = V - L$ is the net flow in the column section. Positive Δ characterizes an equivalent rectifying section, whereas $\Delta < 0$ in an equivalent stripping section. Unfortunately, tray numbers tend to infinity in pinch regions and the problem size is prohibitive for inverse design problems. Therefore, the temperature collocation[11] transforms the continuous column profile equations in terms of stage number, n, into a new composition profile with respect to bubble point temperature, T, as new independent integration variable as shown in Eq. 2. This thermodynamic transformation circumvents the deficiencies of tray numbers as a design variable in inverse network synthesis problems.

Table 1. Thermodynamic Properties of Alkane Mixture Used to Compute the Partial Vapor Pressure by Antoine Equation

Components (x_A, x_B, x_C, x_D)	[Pentane, Hexane, Heptane, Octane]
Antoine Parameter *A*	[6.85221; 6.8702; 6.8938; 6.9094]
Antoine Parameter *B*	[1064.630; 1168.7; 1264.4; 1349.8]
Antoine Parameter *C*	[232.000; 224.2100; 216.6360; 209.3850]

$\log_{10}[P\ (\text{mm Hg})] = A - B/[(T°\text{C}) + C]$.

$$\frac{\partial x_j}{\partial T} = -\frac{\left[\left(1+\frac{1}{R_\Delta}\right)(x_j - y_j) + \frac{1}{R_\Delta}\left(X_{\Delta j} - x_j\right)\right]}{\sum_{j=1}^{c}\left\{\left[\left(1+\frac{1}{R_\Delta}\right)(x_j - y_j) + \frac{1}{R_\Delta}\left(X_{\Delta j} - x_j\right)\right]K_j\right\}}\sum_{j=1}^{c}\frac{\partial K_j}{\partial T}x_j. \quad (2)$$

Thus, liquid composition profiles are computed for any column section. The profile equations are solved for each species j, by global collocation of orthogonal polynomials over finite elements with temperature as independent variable. A detailed derivation, including the nonideal and azeotropic versions of Eq. 2, the temperature, composition, and pressure differential expressions for the phase equilibrium relationship, K_j, are given elsewhere.[11]

Bubble point distance and global feasibility test

For fixed specifications, the bubble point distance is defined as the globally minimum Euclidean distance between the liquid composition profiles of two adjacent column sections. According to this definition, a complex column k is feasible, if and only if the sum of all minimum profile distances of any pair of equivalent rectifying, r, and stripping, s, column sections is within a small ε-tolerance of zero, as in expression (3).

The concept of the Euclidean distance between liquid compositions at an equilibrium stage defined as the bubble point distance is depicted more clearly in Figure 1. It shows a ternary complex column made up of four sections alternating between equivalent rectifying and stripping sections depicted in blue and red, respectively. From the three product nodes, P_1–P_2–P_3, the complex profiles are drawn using

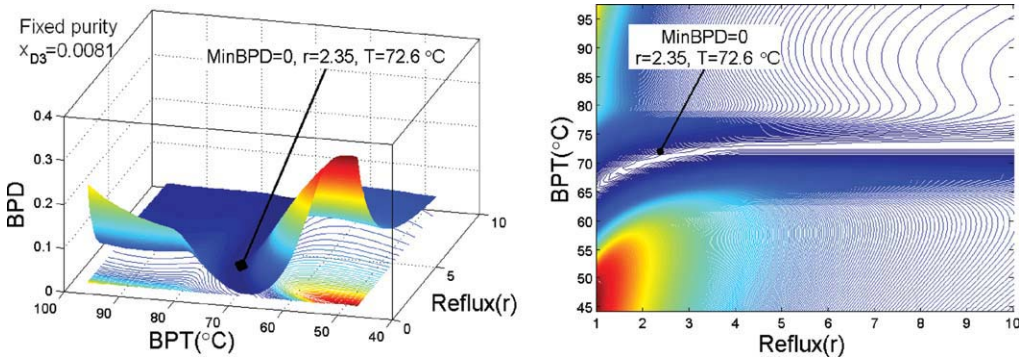

Figure 2. Global minimum BPD search in the reflux ratio space with fixed purity of $x_{D3} = 0.0081$, where a global minimum BPD (10^{-8}) is found at $r = 2.35$.

[Color figure can be viewed in the online issue, which is available at wileyonlinelibrary.com.]

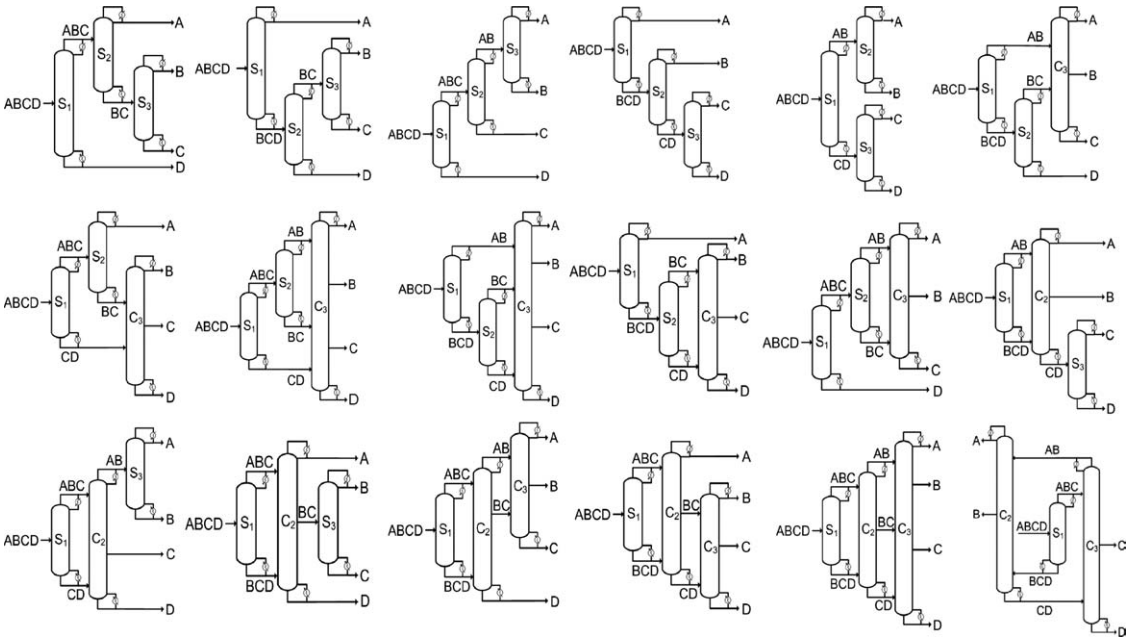

Figure 3. Separation flowsheets to separate a quaternary mixture.

All simple and basic complex configurations are shown.

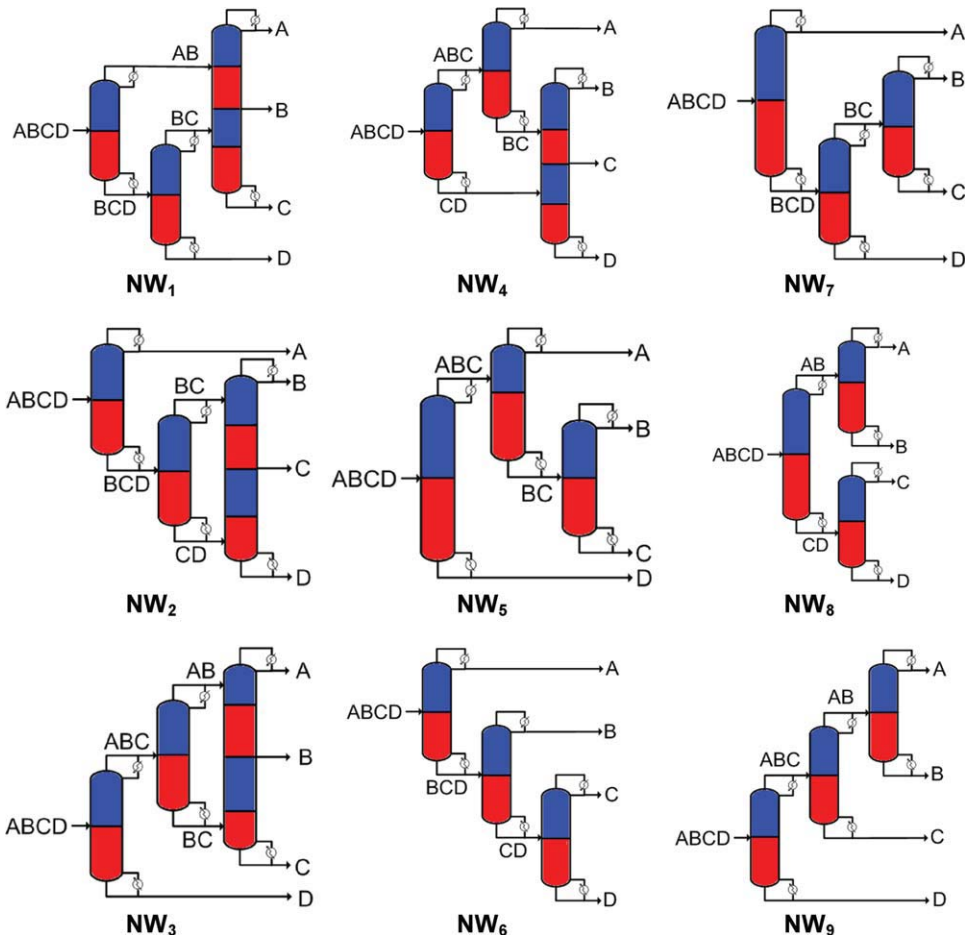

Figure 4. Nine optimal basic network configurations to separate a quaternary mixture.

These configurations have an optimal tradeoff between capital and operating costs, and minimum energy requirement. [Color figure can be viewed in the online issue, which is available at wileyonlinelibrary.com.]

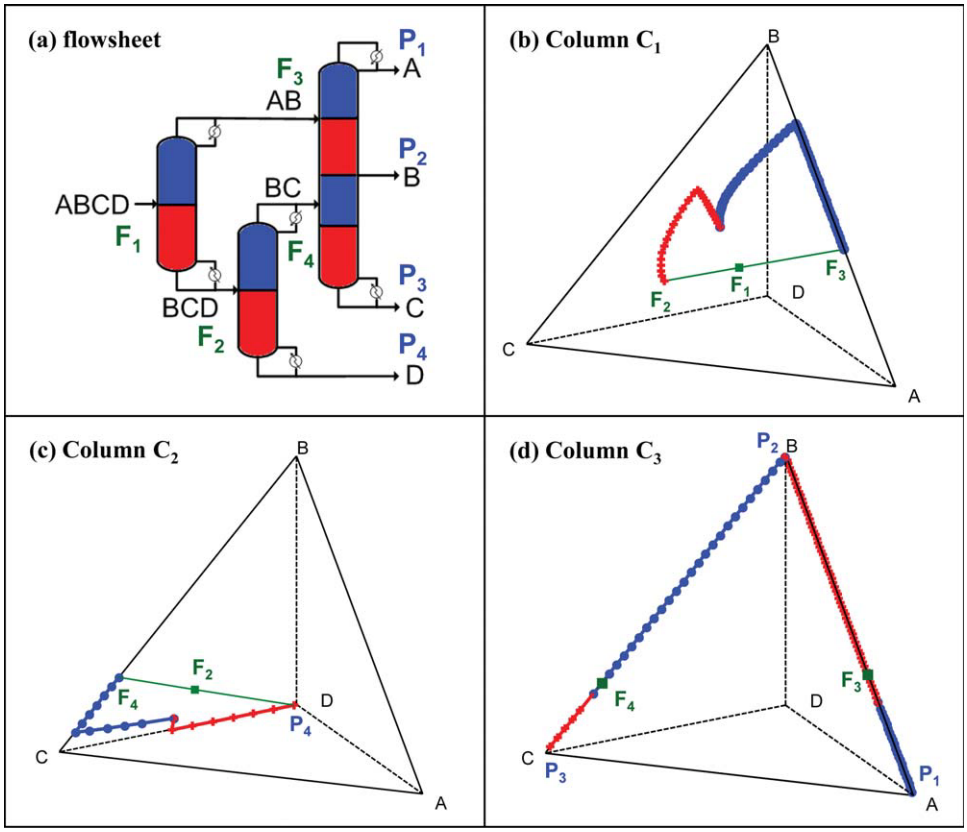

Figure 5. Frame (a) shows the flowsheet with feeds (F1–F4) and products (P1–P4) for the separation of a quaternary mixture.

Frames (b)–(d) represent the tetrahedral composition profiles of columns C1–C3 for the four species *A, B, C*, and *D*. The blue trajectories stand for rectifying sections and red trajectories for stripping section. [Color figure can be viewed in the online issue, which is available at wileyonlinelibrary.com.]

Eq. 2. For a reflux of $r = 2.0$ in Figure 1b, the liquid composition profiles of section S_1 and S_2 exhibit a small gap, this gap is exactly the bubble point distance. Similarly, the gap between the profiles of S_3 and S_4 delineates a nonzero bubble point distance. Accordingly, operating the column with a reflux of $r = 2$ would lead to nonzero bubble point distances between two adjacent column profiles. Therefore, these specifications do not give feasible operating conditions. However, when choosing a reflux of $r = 2.36$, the liquid composition profiles smoothly touch, a situation consistent with a bubble distance of (almost) zero. Hence, a reflux of $r = 2.36$ yields feasible operation. In general, a complex column is feasible if and only if all its adjacent column profiles have a bubble point distance of zero. The sum of all its column section BPD is still a scalar. This value also measures the closeness to an attainable design specification. The ability to judge the closeness of a separation target to realizable specifications is helpful in search algorithms for realizable networks.[12] For a simple or complex column, all its section profiles are computed with the profile equations in (2). The composition trajectories of all species in two adjacent column sections must connect without a gap for a design to be realizable.

An entire separation train is feasible, if and only if all its simple or complex columns, k, are feasible. The network feasibility is given in Eq. 4. Therefore, our network design strategy can be formulated using the following steps: (i) Specify desired product purities and fix open degrees of freedom such as operating conditions (reflux or reboil ratios), (ii) starting from the desired product purities, compute the complex column profiles for equivalent rectifying and stripping sections in each column, (iii) calculate the bubble point distance functions for each pair of adjacent profiles, $\phi(k)$, (iv) conclude that the entire network is feasible if the total

Table 2. Vapor Rate for Each Column and Total Vapor Rate of Each Designed Network

	NW_1	NW_2	NW_3	NW_4	NW_5	NW_6	NW_7	NW_8	NW_9
Col. I (kmol/h)	74.99	79.99	186.87	114.81	186.87	156.56	156.56	478.08	186.87
Col. II (kmol/h)	78.07	57.36	46.73	63.34	60.60	66.44	281.14	63.70	472.62
Col. III (kmol/h)	70.34	64.66	48.99	86.30	62.68	76.09	62.681	72.50	63.27
Total (kmol/h)	223.41	202.02	282.59	264.45	310.15	299.09	500.38	614.28	722.76

Table 3. Column Design Aspects Obtained by Solving the Inverse Design Problem of Nine Column Configurations to Separate a Quaternary Mixture Using the Minimum BPD Design Algorithm

		NW_1	NW_2	NW_3	NW_4	NW_5	NW_6	NW_7	NW_8	NW_9
Column I	Total stages	34	35	44	43	44	95	95	20	44
	Feed stage	21	9	37	40	37	39	39	10	37
	Reflux	0.8	2.17	1.5	0.67	1.5	5.2	5.2	8.6	1.5
Column II	Total stages	70	31	39	40	44	43	28	27	22
	Feed stage	39	9	16	12	15	18	20	11	16
	Reflux	1.36	1.09	0.498	1.51	1.4	1.2	4.68	1.548	8.5
Column III	Total stages	40	50	51	37	36	28	30	38	31
	Feed stage	9	6	10	11	13	11	13	15	13
		33	34	38	31	–	–	–	–	–
	Reflux	1.8	1.6	0.95	1.42	1.53	3.157	1.532	1.889	1.530

In this table, continuous length were converted to actual tray using Eq. 5; remark were rounded to next integer for better comparison with Aspen simulation.

distance is zero, $\Psi(k)$, or modify operating conditions in case a single bubble point distance criterion is violated.

$$\phi(k) = \sum \min \mathrm{BPD}(T) < \varepsilon_1 \tag{3}$$

$$\Psi(k) = \sum_{k=1}^{K} \phi(k) < \varepsilon_2. \tag{4}$$

Illustration: Alkane separation

Consider a simple direct column to take off 99% pentane as distillate from a equimolar alkane mixture of Pentane, Hexane, Heptane, and Octane with vapor–liquid data given in Table 1. Figure 2 illustrates the topology of the thermodynamic BPD search space for different design specifications. With given feed and fixed desired product purities, all four open column degrees of freedom for the quaternary separation problem are fully determined. The reflux, r, now needs to be uniquely determined to meet these design specifications. The reflux, $r = 2.35$, gives the globally minimum BPD; this is the desired operating condition for feasible separations. In some cases, a desired purity target cannot be matched with any reflux. Such a specification is termed infeasible.

Finite element approximation of column profiles

The composition profiles in the illustration were computed using the generalized continuous temperature profiles. Equation 2 was globally discretized with finite element collocation on orthogonal polynomials. The polynomial approximation of the liquid column profiles has the additional advantage that the global optimization problem to compute the minimum BPD can be solved in polynomial arithmetic. Global temperature support combined with polynomial arithmetic guarantee global optimality of the bubble distance minimization for any solution model, ideal, nonideal, and azeotropic. In addition, the computations converge readily for feasible as well as infeasible design specifications.

Results and Applications

Complex network synthesis

Consider again purifying a feed stream of 100 kmol/h (27.78 mol/s) of a quaternary alkane mixture in equimolar fractions of Pentane, Hexane, Heptane, and Octane into products with purity of at least 99%. Agrawal[6] suggested 18 structurally distinct flowsheet configurations including 13 complex configurations shown in Figure 3 to realize this separation task. When also admitting nonbasic configurations without thermal coupling, 24 alternative configurations would have to be considered.[14,15] Here, we wish to explore rigorous designs of a subset of flowsheets for the quaternary separation problem. Because of space limitations, the details of only four complex and five simple network configurations shown in Figure 4 will be presented. For each network, the minimum bubble point distance algorithm was used to determine feasible network specifications that met the final purity constraints. Feasible column profiles were determined using temperature collocation in Eq. 2. Specifications were adjusted until feasibility was achieved with the network BPD criterion in inequalities (3) and (4).

The separation network configuration, NW_1, has three columns. The first column operated as a prefractionator renders sloppy splits and no final products. The second column is a ternary simple column, which yields an indirect split with 99% purity of octane, component D, in the bottom product. The third column consists of four complex column sections generating three product streams at once, top–middle–bottom products.

Figure 5 shows the composition profiles of the entire network with precise intersection between all pairs of adjacent column sections in each distillation tower. For each column section, purities and refluxes had to be suitably adjusted to satisfy the network BPD feasibility criterion. Global BPD minimization was performed with a stochastic global search[12] typically using the third component molar fraction

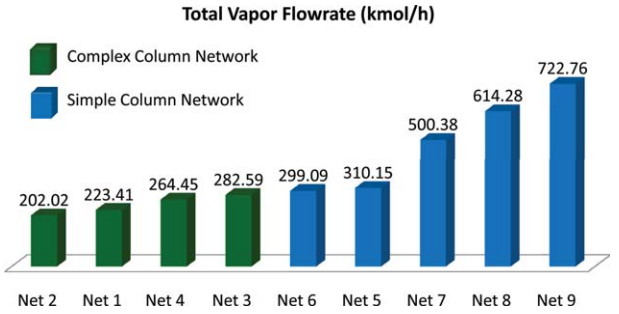

Figure 6. Comparison of the total vapor duty in each distillation network.

In this case study, every complex network required less energy than any of the five simple networks configurations. [Color figure can be viewed in the online issue, which is available at wileyonlinelibrary.com.]

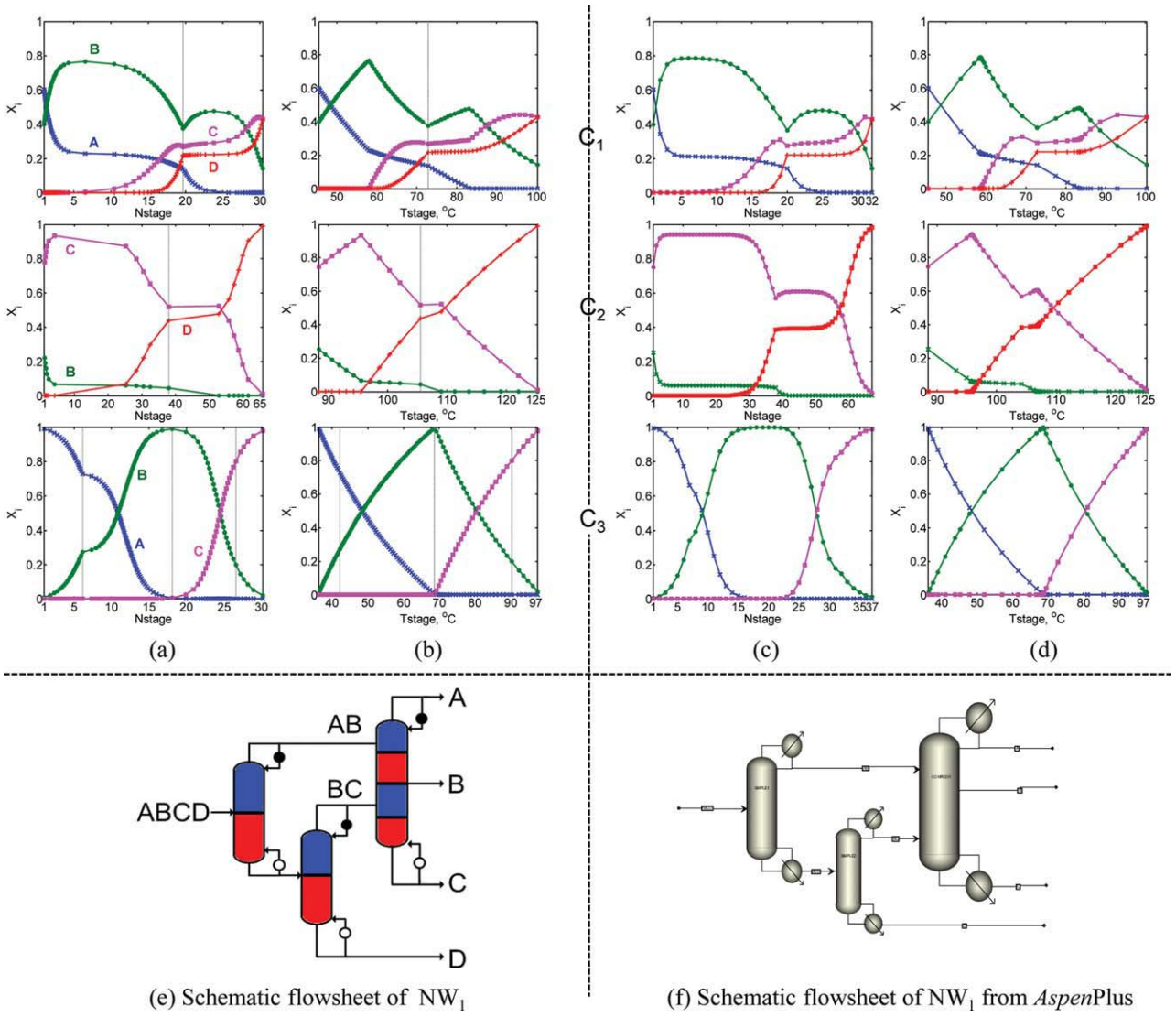

Figure 7. Initialization of AspenPlus by temperature collocation approach to validate network NW_1.

Frames (a) and (b) show the composition profiles of all columns in the stage number and temperature space, respectively, found by temperature collocation. Frames (c) and (d) describe the profiles of the entire network in the stage number and temperature space, respectively, found by AspenPlus. (Remarks: component *A*: blue, --X--; component *B*: green, --●--; component *C*: pink, --■--; component *D*: red, --+--). [Color figure can be viewed in the online issue, which is available at wileyonlinelibrary.com.]

in the distillate product, $x_{3,D}$, and the reflux ratio, r, as the remaining search variable. Purities of internal product cuts such as the distillate and bottoms for the prefractionator column were chosen to lower the total energy consumption. However, currently we offer no claim for rigorous optimality of the various structural solutions of this separation task. Therefore, final conclusions about superior structures have to be deferred to a follow-up article, which will deal with the rigorous global optimization of entire networks.

Note that traditional design methods assuming sharp splits are not suitable for the synthesis of the heat integrated complex networks of Figure 5. Also, the prefractionator is not pinched so that minimum reflux or pinch alignment methods are inadequate for its design. Yet, it will be shown next that prefractionator columns are an essential element in energy-efficient separations, even though they cannot be designed with traditional design approaches.

Energy-efficient separations

All nine network configurations shown in Figure 4 use quaternary columns as direct, indirect, or prefractionator separation units were solved with the temperature collocation method.[11] The initial feed is a saturated liquid; the feeds to subsequent columns include saturated vapor for lower energy consumption. Energy efficiency for each flowsheet was assessed by computing the total vapor flow rate defined as the sum of the individual column vapor flows. Although total vapor rate for the separation network does not account for different temperature levels required in second law analyses, this parameter serves well as a first approximation of total expected energy cost. The total vapor duty required for each of the nine configurations is given in Table 2. Table 3 summarizes the design aspects and configurations of all nine networks computed by our inverse design methodology. The

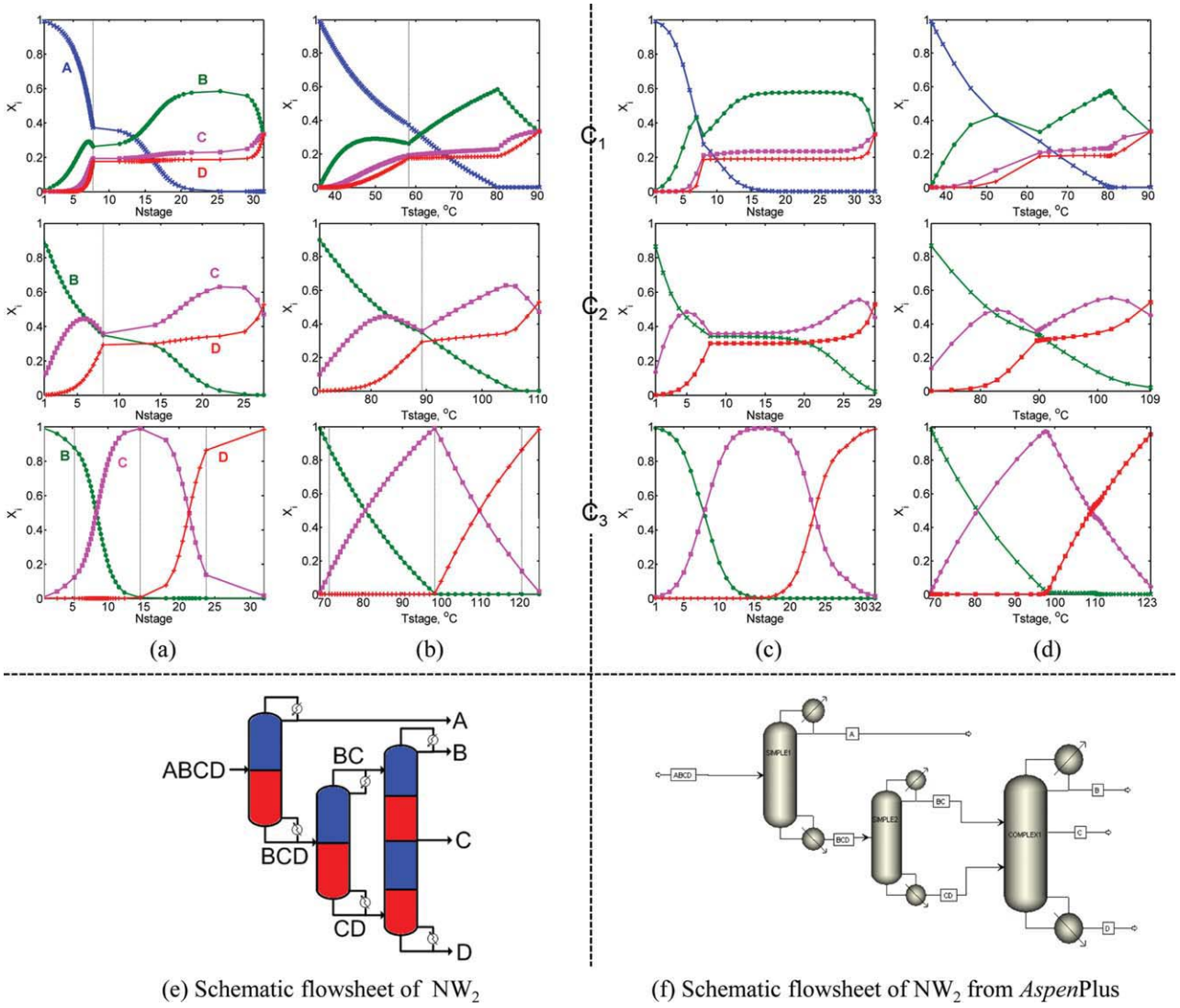

Figure 8. Initialization of AspenPlus by temperature collocation approach to validate network NW_2.

Frames (a) and (b) show the composition profiles of all columns in the stage number and temperature space, respectively, found by temperature collocation. Frames (c) and (d) describe the profiles of the entire network in the stage number and temperature space, respectively, found by AspenPlus. (Remarks: component *A*: blue, --X--; component *B*: green, --●--; component *C*: pink, --■--; component *D*: red, --+--). [Color figure can be viewed in the online issue, which is available at wileyonlinelibrary.com.]

synthesis rigorously synthesized networks leading to the same final product purities.

Figure 6 lists the total vapor flow rate for each separation network. For this feed and thermodynamics of this mixture, networks with complex configurations used less energy than any of the five simple configurations. This result clearly demonstrated the advantages of using sloppy, nonpinched prefractionators instead of classical sharp-split specifications. In this study, network NW_2 is the most energy efficient configuration with a total vapor rate of 56.1 mol/s. The best complex column network, NW_2, used 33% less than the best simple network, NW_6, and 72% less than the worse simple network, NW_9. This result shows how to systematically find the detailed design information for all feasible columns. For such a synthesis result to be of practical value, it should be possible to validate it in the field. Unfortunately, construction projects of new pilot plants or refineries are rare; therefore, we propose to verify our results with a rigorous industrially accepted flowsheet simulator. Accordingly, all energy efficient networks synthesized by temperature collocation presented here will be validated using the rigorous AspenPlus flowsheet simulation software.

Validation of energy-efficient networks with commercial flowsheet simulation

Existing design methodologies do not yield detailed design information to satisfy the rigorous mass, equilibrium, summation, and heat equations (MESH) for separation networks. For example, the Underwood,[16,17] Pinch Alignment,[18] and Rectifying Body methods give idealized pinched columns with infinitely many trays without information about the

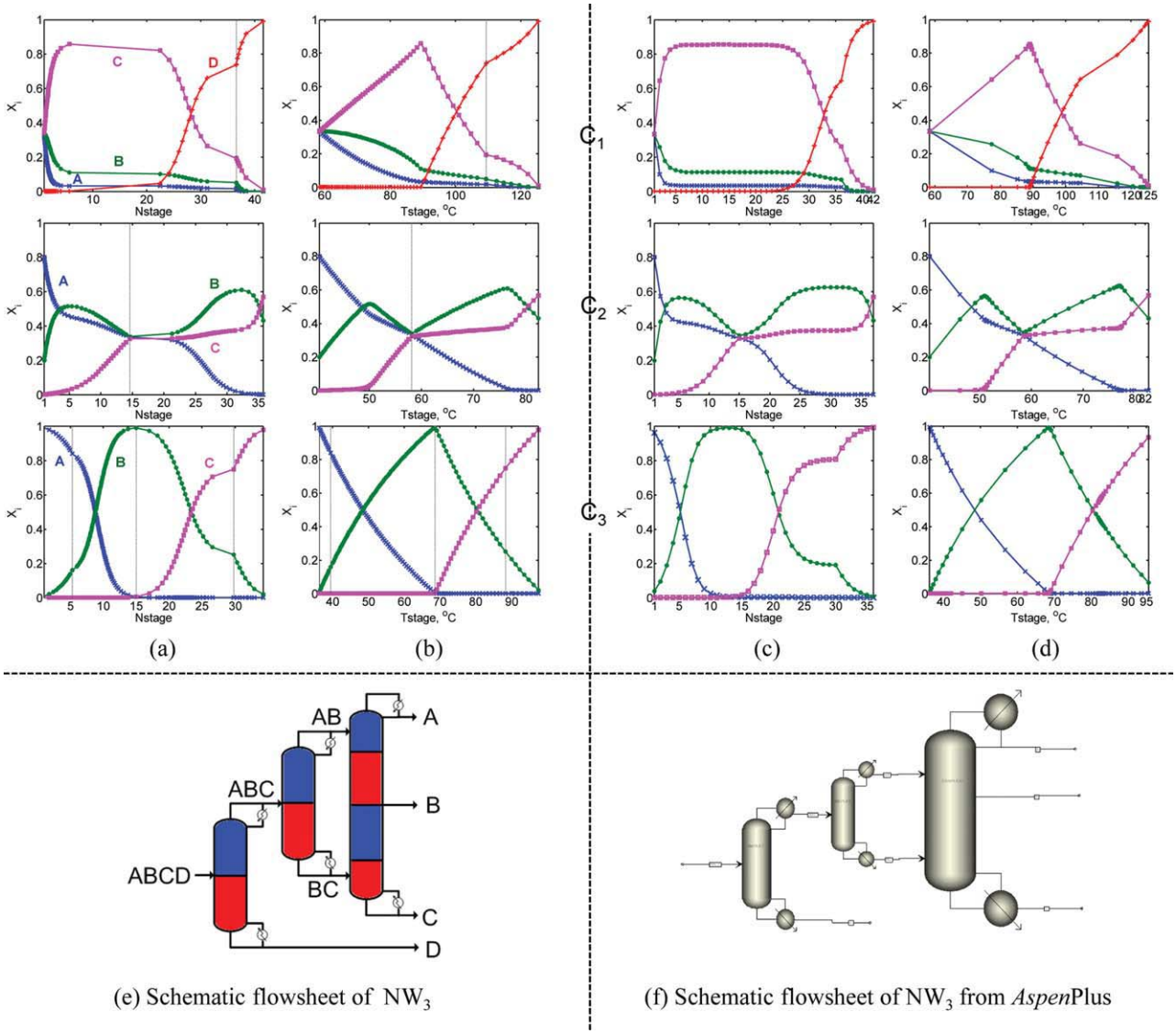

Figure 9. Initialization of AspenPlus by temperature collocation approach to validate network NW_3.

Frames (a) and (b) show the composition profiles of all columns in the stage number and temperature space, respectively, found by temperature collocation. Frames (c) and (d) describe the profiles of the entire network in the stage number and temperature space, respectively, found by AspenPlus. (Remarks: component *A*: blue, --X--; component *B*: green, --●--; component *C*: pink, --■--; component *D*: red, --+--). [Color figure can be viewed in the online issue, which is available at wileyonlinelibrary.com.]

network stage connectivity of the multifeed and multiproduct flowsheet, its specific operating conditions such as vapor and liquid flows and composition profiles. Accordingly, the limiting assumptions of these design methods do not help in validating process designs with rigorous flowsheet simulations. Aspects such as multifeed location and the position of side-product trays are critical information that any process simulator needs in its basic setup.

In contrast to the restrictions of the conventional design methodologies, our approach rigorously computes all liquid and vapor profiles resulting from the predicted operating conditions such as reflux and reboil ratios, total tray numbers, and the location of product removal streams for all column sections, and a stream table of all intermediate and final products. Once compositions profiles of the entire network have been calculated as a function of temperature, the column height can easily be recovered by back transformation from temperature to stage number as in Eq. 5. Integration of the column profiles from the top to the bottom stage gives the number of equilibrium stages, n. The number of stages is also needed in capital cost estimation.

$$\frac{dn}{dT} = \frac{\partial n}{\partial x_j}\frac{\partial x_j}{\partial T} = -\frac{\sum_{j=1}^{c}\frac{\partial K_j}{\partial T}x_j}{\sum_{j=1}^{c}\left\{\left[\left(1+\frac{1}{R_\Delta}\right)(x_j-y_j)+\frac{1}{R_\Delta}\left(X_{\Delta j}-x_j\right)\right]K_j\right\}}. \quad (5)$$

Table 3 summarizes the detailed design aspects and specifications of all nine networks computed by our inverse synthesis method. This detailed network specifications are used

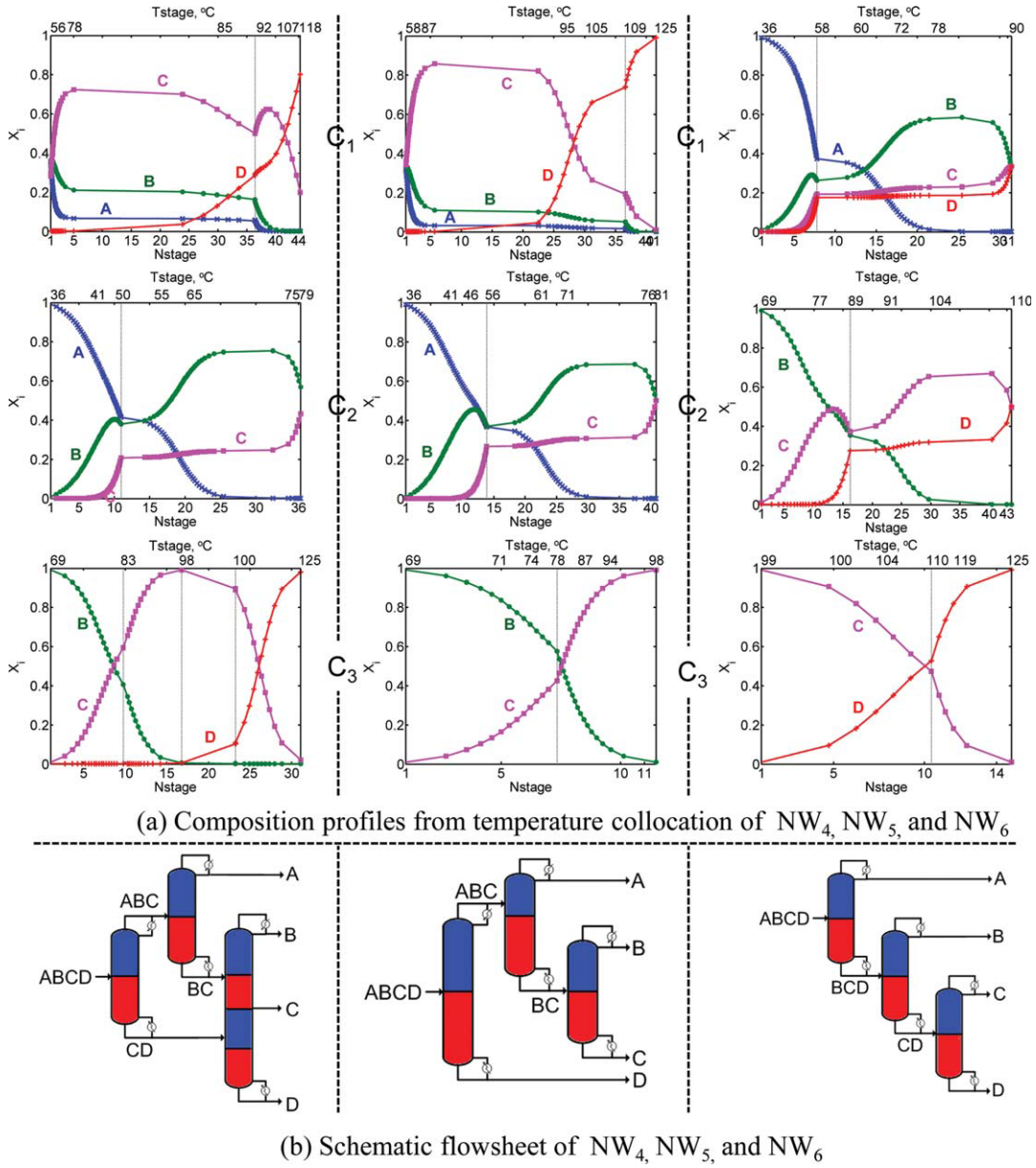

Figure 10. Composition profiles vs. number of stages and temperature stage domains found by temperature collocation for networks NW_4, NW_5, and NW_6.

Frame (a) shows the composition profiles of all columns in the stage number and temperature space for NW_4, NW_5, and NW_6. Frame (b) contains the schematic flowsheet diagrams for all three networks. (Remarks: component *A*: blue, --X--; component *B*: green, --●--; component *C*: pink, --■--; component *D*: red, --+--). [Color figure can be viewed in the online issue, which is available at wileyonlinelibrary.com.]

to initialize an equivalent AspenPlus flowsheet. The Aspen performance calculation converged typically within a couple of iterations in a few CPU seconds, thus confirming essential agreement between the two computational results. The predicted column profiles of columns in networks NW_1, NW_2, and NW_3 from our temperature collocation method are compared to the Aspen profiles in Figures 7–9, respectively. The graphs show the evolution of the liquid composition profiles as a function of bubble temperature, Tstage, as well as in terms of stage number, Nstage. The mean error between the profiles obtained via the inverse and the rating problem is less than a few percent. The difference is larger in the middle sections of the columns, but virtually the same purities are obtained at the product nodes. In the case studies reported here, the differences between the Aspen predictions and our profile computations did not exceed 5%. The deviation at the products nodes was typically less of 0.1%. Such small concentration differences are below the accuracy of standard concentration measurement in the industrial practice, but may be significant in ultrapure gas separations. These cases can be dealt with by a suitable tightening of the bubble point tolerances. We found the agreement between our inverse designs with AspenPlus simulations remarkable, despite qualitative differences between the continuous generalized profile equations used in temperature collocation vs. the tray-by-tray computations in flowsheet simulators. Six

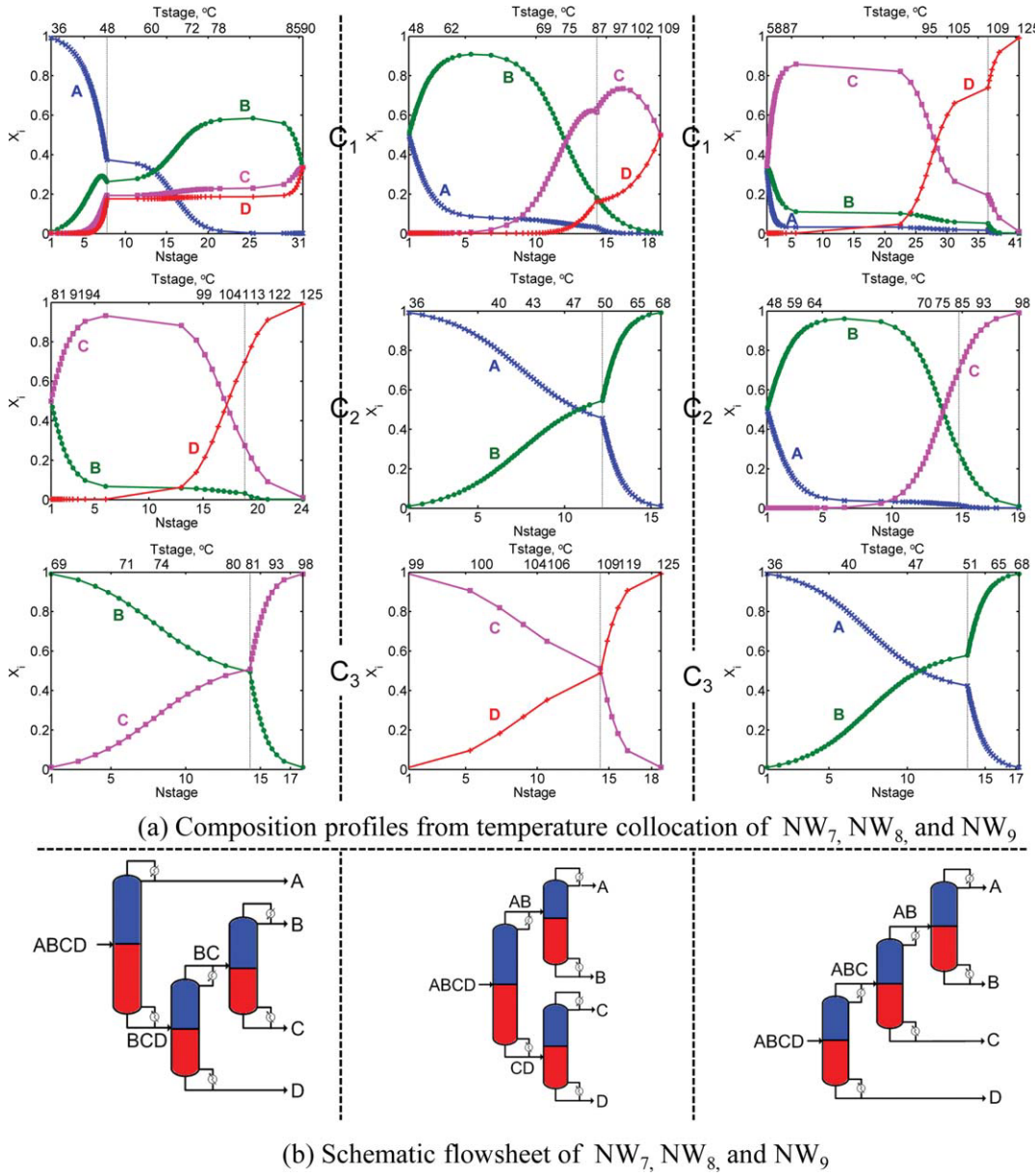

Figure 11. Composition profiles vs. number of stages and temperature stage domains found by temperature collocation for networks NW_7, NW_8, and NW_9.

Frame (a) shows the composition profiles of all columns in the stage number and temperature space for NW_7, NW_8, and NW_9. Frame (b) shows the schematic flowsheet for each network. (Remarks: component *A*: blue, --+--; component *B*: green, --X--; component *C*: pink, --●--; component *D*: red, --■--). [Color figure can be viewed in the online issue, which is available at wileyonlinelibrary.com.]

other network configurations were also validated. We only show the composition profiles from temperature collocation results of networks NW_4–NW_9 in Figures 10 and 11 for the sake of brevity. A critical comparison confirmed the excellent agreement between our synthesis results and the precise Aspen validation.

Discussion

Temperature collocation elucidates the topology of the search space for identifying feasible operating conditions in multicomponent separations. The globally optimal BPD function reflects feasibility of the separation target. If its magnitude is close to zero, the design specifications are realizable, otherwise they cannot be realized. In practice, a small tolerance such as $\|\mathrm{BPD}\| \leq 10^{-4}$ may be a suitable close-to-zero criterion. The results of Figure 2 also depict a narrow canyon delineating a spectrum of reflux designs with almost zero BPD, $10^{-6} < \mathrm{BPD} < 10^{-3}$. Such a small difference would not be detectable when solving algebraically the mass, equilibrium, summation, and heat equations (MESH), with tolerances enforced for each tray balance of similar magnitude. This phenomenon explains why several earlier

publications have shown columns with different refluxes and tray numbers for almost identical products. Two designs in the narrow canyon of the BPD space are indistinguishable using a rigorous MESH solving algorithm. Our method, however, clearly discriminates between different reflux alternatives, where the BPD is almost zero.

For energy efficient design, we found that networks involving complex column configurations required 30–70% less total vapor than simple sequences. Complex networks may also perform sloppy and nonpinched splits as needed to achieve the overall separation target with low energy consumption. Nonsharp and nonpinched complex columns are not amenable to most traditional design methods.

This study also demonstrated the possibility to initialize and validate our synthesized design solutions with rigorous flowsheet simulations. A close agreement between the temperature collocation results and the Aspen simulation results was observed and visualized in the bubble point temperature domain.

Conclusions

This article shows the generalization of the minimum bubble point distance algorithm to design energy efficient complex separation networks. The temperature continuous difference point equations were used to compute the liquid composition trajectories of complex and simple network configurations. The robustness of the design algorithm was demonstrated by designing feasible configurations to realize both sharp and sloppy purity requirements.

The minimum bubble point distance measurement was robust and efficient to find detailed network specifications guaranteeing the feasibility criterion of exact profile intersection. The thermodynamically motivated bubble temperature transformation offers massive size reduction for simple and complex column profile computations, eliminates singularities in the conventional composition profiles near stationary and saddle pinch points, extends to any dimension of multicomponent mixture with any phase equilibrium relationship such as constant relative volatility, ideal, and nonideal mixtures, and applies to both sharp and sloppy splits.

This study demonstrates its robustness for proposed separation synthesis approach. In this article, nine column networks were designed in detail to separate a quaternary alkane mixture. Four complex and five simple network configurations were studied in detail. In this case, all four complex networks use less vapor duty than any possible simple network configuration. The best complex column network used 33% less vapor rate than the best simple network.

Finally, the last section demonstrated a remarkable agreement between the inverse design solutions and rigorous forward flowsheet simulations. The optimal feasible designs were validated by initialization of AspenPlus[19] simulations, which converged in a few iterations. The mean deviation between the profiles obtained via the inverse and the rigorous forward or performance calculations problem was smaller than standard concentration measurement common in the industrial practice. This excellent agreement demonstrates the practicability of our inverse problem solution. It can also be used to set up large or complex separation problems on rigorous flowsheet simulators. Our findings also suggest that potential energy savings can be realized when systematically exploring complex synthesis to solve industrial separation problems.

Acknowledgments

Financial support by DOE Grant: DE-FG36-06GO16104 is gratefully acknowledged. The authors appreciate helpful discussion with Dr. R. Agrawal on complex columns. Ms. Laura Moes participated in the UIC REU program NSF EEC 0754590 and REU Supplement NSF CBET-0626162. We acknowledge Dr. Chau-Chyun Chen for his support providing an Aspen software research license.

Literature Cited

1. Doherty MF, Malone MF. *Conceptual Design of Distillation Systems*. McGraw-Hill: New York, NY, 2001:568.
2. Van Dongen DB, Doherty MF. Design and synthesis of homogeneous azeotropic distillations. 1. Problem formulation for a single column. *Ind Eng Chem Fundamentals*. 1985;24:454–463.
3. Marquardt W, Kossack S, Kraemer K. A framework for the systematic design of hybrid separation processes. *Chinese J Chem Eng*. 2008;16:333–342.
4. Holland ST, Tapp M, Hildebrandt D, Glasser D. Column profile maps. 2. Singular points and phase diagram behavior in ideal and nonideal systems. *Ind Eng Chem Res*. 2004;43:3590–3603.
5. Agrawal R, Fidkowski ZT. Are thermally coupled distillation columns always thermodynamically more efficient for ternary distillations? *Ind Eng Chem Res*. 1998;37:3444–3454.
6. Agrawal R. Synthesis of multicomponent distillation column configurations. *AIChE J*. 2003;49:379–401.
7. Lucia A, Taylor R. The geometry of separation boundaries. II. Mathematical formalism. *AIChE J*. 2007;53:1779–1788.
8. Lucia A, Taylor R. The geometry of separation boundaries: I. Basic theory and numerical support. *AIChE J*. 2006;52:582–594.
9. Lucia A, Amale A, Taylor R. Distillation pinch points and more. *Comput Chem Eng*. 2008;32:1350–1372.
10. Tapp M, Holland ST, Hildebrandt D, Glasser D. Column profile maps. 1. Derivation and interpretation. *Ind Eng Chem Res*. 2004;43:364–374.
11. Zhang L, Linninger AA. Temperature collocation algorithm for fast and robust distillation design. *Ind Eng Chem Res*. 2004;43:3163–3182.
12. Zhang L, Linninger AA. Towards computer-aided separation synthesis. *AIChE J*. 2006;52:1392–1409.
13. Ruiz GJ, Kim S, Moon J, Zhang L, Linninger AA. Design and Optimization of Energy Efficient Complex Separation Networks. Seventh International Conference on the Foundations of Computer-Aided Process Design, 2009; Taylor & Francis Group, 2009:747–745.
14. Giridhar A, Agrawal R. Synthesis of distillation configurations: I. Characteristics of a good search space. *Comput Chem Eng*. 2010;34:73–83.
15. Giridhar A, Agrawal R. Synthesis of distillation configurations. II: A search formulation for basic configurations. *Comput Chem Eng*. 2010;34:84–95.
16. Underwood AJV. Fractional distillation of ternary mixtures: part I. *Inst Petrol J*. 1945;31:111–118.
17. Underwood AJV. Fractional distillation of ternary mixtures: part II. *Inst Petrol J*. 1946;32:598–613.
18. Julka V, Doherty MF. Geometric behavior and minimum flows for nonideal multicomponent distillation. *Chem Eng Sci*. 1990;45:1801–1822.
19. AspenTech. AspenPlus. Available at: http://www.aspentech.com. 2009.

Appendix: Finite Element Approximation of Column Profiles

This Appendix reviews in brevity the mathematical background for temperature collocation. The main advantage is the use of temperature instead of stage numbers. The

temperature is a better choice, because (i) the independent variable is defined within well-defined bounds (that is the bubble points temperatures of the pinch points), (ii) the bubble point temperature of the stable pinch points can be found before executing rigorous profile computations, and (iii) temperature integration can traverse regions that are pinched in terms of tray numbers. A detailed description is beyond the scope of this article, but can be found in earlier publication of our group.[11]

We use a global integration strategy to solve the continuous model equations to compute the liquid composition profiles using Eq. A1. The finite elements collocation uses compact polynomial sets to represent the composition profiles for each species over the specified temperature ranges known as an element. Several elements—typically in the order of five—make up an entire column section. The entire range from the product node to the stable pinch point is thus continuously covered. It is also critical to place element boundaries on saddle pinch temperatures to better cover sharp composition changes and curvature of the profiles occurring typically near node temperatures.[11] By this informed placement of final elements boundaries and choices for the number of nodes, the highly accurate composition profiles can be computed over the entire temperature range from the product purity all the way down to the stable pinch point.

For the profile equations (A1) with finite temperature elements and collocation on orthogonal polynomials (OCFE), Lagrange interpolation polynomials are used.

$$\frac{\partial x_j}{\partial T} = -\frac{\left(\left(1+\frac{1}{R_\Delta}\right)(x_j-y_j)+\frac{1}{R_\Delta}\left(X_{\Delta j}-x_j\right)\right)}{\sum_{j=1}^{c}\left[\left(\left(1+\frac{1}{R_\Delta}\right)(x_j-y_j)+\frac{1}{R_\Delta}\left(X_{\Delta j}-x_j\right)\right)K_j\right]}\sum_{j=1}^{c}\left(\frac{\partial K_j}{\partial T}x_j\right) = g(x,T). \quad \text{(A1)}$$

This OCFE discretization gives a nonlinear algebraic equation system where the unknown variables are the unknown weights (compositions) at each collocation node. The derivatives of node n in element e leads to Eq. A2,

$$\left.\frac{d\mathbf{x}}{dT}\right|_{T=T_n^e} = \mathbf{A}_{T_n^e}\mathbf{x}_{n,c}^e \quad \text{(A2)}$$

$\mathbf{x}_{n,c}^e$ is the vector of unknown composition of each species c at node n in element e at temperature T_n^e. The right-hand side of Eq. A2 is represented by the nonlinear functions, $g(x,T)$; these functions in Eq. A3 are nonlinear because of the nonlinear equilibrium model relating the liquid and vapor compositions.

$$A\mathbf{x} = g(x,T). \quad \text{(A3)}$$

System (A3) is a nonlinear algebraic system that is solved with a suitable algorithm such as Newton methods with line search.[11,12]

Manuscript received Nov. 25, 2009, and revision received Feb. 10, 2010.